

Progresses on Th-doped materials for solid-state nuclear clock

Cheng-Chun Zhao(赵呈春), Lin Li(李琳), Shan-Ming Li(李善明), Qiao-Rui Gong(龚巧瑞), Pei-Xiong Zhang(张沛雄), Yin Hang(杭寅), Long-Sheng Ma(马龙生), and Shi-Ning Zhu(祝世宁)
Citation: Chin. Phys. B, 2026, 35 (**2**): 020602. DOI: 10.1088/1674-1056/ae210f
http://cpb.iphy.ac.cn; http://iopscience.iop.org/cpb

What follows is a list of articles you may be interested in

Progresses on 148 nm light sources for precision measurement of nuclear transition of ^{229m}Th

Yang Wang(王样), Zheng-Rong Xiao(肖峥嵘), Heng-Zhi Zhang(张恒之), Lin-Qiang Hua(华林强), and Xiao-Jun Liu(柳晓军)
Chin. Phys. B, 2026, 35 (**2**): 020601. DOI: 10.1088/1674-1056/ae0d78

A Yb optical clock with a lattice power enhancement cavity

Chunyun Wang(王春云), Yuan Yao(姚远), Haosen Shi(师浩森), Hongfu Yu(于洪浮),Longsheng Ma(马龙生), and Yanyi Jiang(蒋燕义)
Chin. Phys. B, 2024, 33 (**3**): 030601. DOI: 10.1088/1674-1056/ad1986

Sympathetic electromagnetically induced transparency ground state cooling of a $^{40}Ca^{+}$–$^{27}Al^{+}$ pair in an $^{27}Al^{+}$ clock

Chenglong Sun(孙成龙), Kaifeng Cui(崔凯枫), Sijia Chao(晁思嘉), Yuanfei Wei(魏远飞), Jinbo Yuan(袁金波), Jian Cao(曹健), Hualin Shu(舒华林), and Xueren Huang(黄学人)
Chin. Phys. B, 2023, 32 (**5**): 050601. DOI: 10.1088/1674-1056/aca39d

Laboratory demonstration of geopotential measurement using transportable optical clocks

Dao-Xin Liu(刘道信), Jian Cao(曹健), Jin-Bo Yuan(袁金波), Kai-Feng Cui(崔凯枫), Yi Yuan(袁易),Ping Zhang(张平), Si-Jia Chao(晁思嘉), Hua-Lin Shu(舒华林), and Xue-Ren Huang(黄学人)
Chin. Phys. B, 2023, 32 (**1**): 010601. DOI: 10.1088/1674-1056/ac6337

Study of optical clocks based on ultracold ^{171}Yb atoms

Di Ai(艾迪), Hao Qiao(谯皓), Shuang Zhang(张爽), Li-Meng Luo(骆莉梦), Chang-Yue Sun(孙常越), Sheng Zhang(张胜), Cheng-Quan Peng(彭成权), Qi-Chao Qi(齐启超), Tao-Yun Jin(金涛镭), Min Zhou(周敏), Xin-Ye Xu(徐信业)
Chin. Phys. B, 2020, 29 (**9**): 090601. DOI: 10.1088/1674-1056/aba099

TOPICAL REVIEW — Advances in thorium nuclear optical clocks

Progresses on Th-doped materials for solid-state nuclear clock

Cheng-Chun Zhao(赵呈春)[1,2], Lin Li(李琳)[1,2], Shan-Ming Li(李善明)[1,2], Qiao-Rui Gong(龚巧瑞)[1,2], Pei-Xiong Zhang(张沛雄)[1,3,†], Yin Hang(杭寅)[1,2,‡], Long-Sheng Ma(马龙生)[4], and Shi-Ning Zhu(祝世宁)[5]

[1] *Research Center of Laser Crystal, Shanghai Institute of Optics and Fine Mechanics, Chinese Academy of Sciences, Shanghai* 201800, *China*
[2] *Center of Materials Science and Optoelectronics Engineering, University of Chinese Academy of Sciences, Beijing* 100049, *China*
[3] *Department of Optoelectronic Engineering, Jinan University, Guangzhou* 510632, *China*
[4] *State Key Laboratory of Precision Spectroscopy, East China Normal University, Shanghai* 200062, *China*
[5] *National Laboratory of Solid-State Microstructures, School of Physics, Collaborative Innovation Center of Advanced Microstructures, Nanjing University, Nanjing* 210093, *China*

(Received 31 August 2025; revised manuscript received 14 November 2025; accepted manuscript online 19 November 2025)

The isomeric transition of thorium-229 (^{229}Th), as the only known laser-accessible nuclear transition, offers the possibility for the development of a new generation of optical clocks. Solid-state nuclear optical clock based on ^{229}Th-doped crystals or thin films has attracted much attention due to its potential advantages in high stability, miniaturization, and robustness. This paper reviews the research progress of solid-state nuclear optical clock materials, analyzes the preparation, defects, and properties of the candidate solid material systems for ^{229}Th, explores the influence of the local crystal environment on the nuclear transition, focuses on introducing the latest research results of crystal materials such as Th-doped CaF_2 and $LiSrAlF_6$, and looks forward to the future development direction of this field. It could provide a reference for the material selection and optimization of solid-state nuclear optical clocks.

Keywords: thorium-229, optical clock, Th-doped crystal, Th-doped film

PACS: 06.30.Ft, 91.60.Ed, 91.60.Mk

DOI: 10.1088/1674-1056/ae210f **CSTR:** 32038.14.CPB.ae210f

1. Introduction

The ^{229}Th isotope has been the subject of extensive scientific research for decades because it possesses a low-energy isomeric nuclear transition at about 8.4 eV ($\sim$ 148.4 nm), which can be excited with tabletop vacuum-ultraviolet (VUV) laser systems.[1,2] The nuclear transition from the isomeric state (^{229m}Th) to the ground state (^{229g}Th) exhibits low sensitivity to environmental perturbations and possesses an extremely narrow natural linewidth. It provides an opportunity for the development of a nuclear optical clock with very high accuracy.[3–6] There are two main approaches to construct such nuclear optical clocks with two different physical implementations. One is $^{229}Th^{3+}$ in an ion trap like that of atomic optical clocks,[5,7] while the other is $^{229}Th^{4+}$ doped VUV-transparent crystal.[8,9] The former scheme can exhibit higher accuracy. The advantage of the latter "solid-state nuclear clock" is a larger signal-to-noise ratio and an improved stability due to the much larger number of ^{229}Th nuclei (up to 10^{18} cm^{-3}) interrogated simultaneously.[10,11] Furthermore, the solid-state nuclear optical clocks do not require large cold-atom systems. Their core components can be ^{229}Th doped crystals/films in millimeter or even micrometer sizes, which has great potential in miniaturization, on-chip integration, and space-borne applications.[12,13]

The development of a solid-state nuclear clock requires ^{229}Th-doped crystals with high VUV transmittance, low background luminescent noise, high radiation damage resistance, as well as highly efficient, low loss, and uniform doping of ^{229}Th. It is difficult to fabricate ^{229}Th-doped crystals because ^{229}Th has extreme toxicity and strong radioactivity. Moreover, ^{229}Th is extremely scarce and expensive because it does not naturally exist, and currently the only way to obtain even microgram ^{229}Th is the α-decay of ^{233}U, which is also a non-natural radioactive material.[8,14] The natural thorium (^{232}Th) is very low in radioactivity and easy to obtain, and has the same extranuclear electron configuration and chemical properties with ^{229}Th. Therefore, ^{232}Th was used formally in most studies on the development of Th doped crystals.[8] Currently, the experimentally reported Th-doped or Th-based solid materials mainly include $NaYF_4$, $LiYF_4$, Na_2ThF_6, $LiCaAlF_6$, $LiSrAlF_6$, $BaLiF_3$, MgF_2, CaF_2, LiF, and SrF_2, whereas only CaF_2, $LiSrAlF_6$, MgF_2, ThF_4 and ThO_2 have used ^{229}Th.[8,15–23] In recent years, rapid progress has been made using ^{229}Th-based solid-state materials. Direct laser excitation and measurement of the nuclear clock transition were demonstrated; subsequently, high-precision spec-

†Corresponding author. E-mail: pxzhang@jnu.edu.cn
‡Corresponding author. E-mail: yhang@siom.ac.cn

© 2026 Chinese Physical Society and IOP Publishing Ltd. All rights, including for text and data mining, AI training, and similar technologies, are reserved.

troscopy was performed, determining the transition frequency with kHz level precision; then, laser excitation was observed in $^{229}ThF_4$ and $^{229}ThO_2$ films.[1,2,22,23]

There are various defects in thorium-doped crystals. Due to the difference in ionic radius and valence state between thorium ions and the substituted metal cations, thorium doping usually causes lattice distortion and produces charge-compensating defects. High-energy rays (e.g., α rays) produced by ^{229}Th nuclear decay damage the crystal lattice and create defects.[16] Defects also form under VUV laser irradiation. These defects can reduce optical transmittance and increase background luminescence. Although the ^{229}Th nuclear transition is environmentally insensitive, the lattice field environment and defects still affect nuclear energy levels and transition decay rates, leading to energy level splitting, line broadening, and lifetime reduction. These factors require in-depth investigation during the development of thorium-doped crystal materials.

Here, we will review the research progress of solid-state nuclear optical clock materials, summarize the material requirements and candidate materials for solid-state nuclear optical clocks, and analyze material defects, and the influence mechanisms of the local material environment on nuclear transitions. It could provide a reference for the design and optimization of solid-state nuclear clock materials.

2. Material requirements for ^{229}Th solid-state nuclear clocks

The construction of ^{229}Th solid-state nuclear clocks requires high demands on the host materials. It is essential for them to possess high VUV transmittance, wide bandgap, high doping compatibility, low luminescent noise, and high radiation resistance stability. The host must maintain a high level of transmittance in the VUV band to allow the excitation and detection of nuclear transition signal. In addition, the bandgap energy must exceed the energy of the ^{229m}Th transition to prevent absorption of the excitation light by electronic transitions. Prominent candidate materials such as CaF_2 (bandgap 11.8 eV) and $LiSrAlF_6$ (bandgap 12 eV) both fulfill this demand.[1,15] Due to the scarcity and high cost of ^{229}Th, it is necessary for a host to have high doping compatibility of Th^{4+} ions. Th^{4+} ions need to be incorporated into the crystal lattice at high concentrations without inducing significant optical degradation. Doping efficiency is influenced by ionic radius matching and charge compensation schemes. For example, Th^{4+} ions (ionic radius 1.19 Å, 8-coordinate) typically substitute for divalent cation sites (Ca^{2+} (ionic radius 1.26 Å, 8-coordinate), Sr^{2+} (ionic radius 1.40 Å, 8-coordinate)), accompanied by charge compensation mechanisms such as interstitial F^- ions. The effective segregation coefficient of Th in SrF_2 is close to 1, enabling high doping uniformity.[20]

The host should exhibit low luminescence noise and high radiation resistance stability. Crystal defects introduce non-radiative decay channels (e.g., internal conversion) and background luminescence. Point defect concentrations (vacancies, interstitials) and impurities must be meticulously controlled. For instance, fluorine vacancies (V_k centers) in CaF_2 can trap electrons and form absorption centers. In addition, the decay of ^{229}Th (half-life 7880 years) emits α particles, which causes permanent radiation damage to crystals. Selecting radiation-tolerant materials is a fundamental solution to this issue, although experiments demonstrate that superionic state fluorine annealing effectively repairs radiation damage in CaF_2.[24]

In the decay chain of ^{229}Th, five α particles are emitted with energies higher than 5 MeV. In crystals, the decay of ^{229}Th produces high-energy radiation (e.g., α, β, γ rays).[25] These rays transfer energy to atoms within the crystal, causing atoms to dislodge from their equilibrium lattice positions and form point defects or complex defects. Therefore, crystals doped with ^{229}Th must possess good resistance to radiation damage. The radiation tolerance of fluoride crystals is influenced by several key material factors such as defect formation energy and structural stability under irradiation. The defect formation energy is the minimum energy required to remove an atom from a perfect crystal and form a defect, directly determining the difficulty of defect generation under irradiation. A higher defect formation energy results in a lower concentration of irradiation-induced defects and stronger radiation resistance of the crystal. The defect formation energy of fluoride crystals is mainly influenced by ionic bond strength and lattice energy. In fluoride crystals, fluoride ions are more likely to be displaced from the lattice than metal cations, forming fluoride vacancies and interstitial fluorides. Fluoride crystals with higher fluoride vacancy formation energy exhibit stronger radiation resistance. On the other hand, even if defects are generated by irradiation, if the crystal structure has high stability, characterized by high tolerance for lattice distortion and high energy barriers for defect diffusion, defects will struggle to migrate and agglomerate. In other words, stronger structural stability means that irradiation-induced point defects are more likely to be pinned locally, leading to slower degradation of crystal performance. For instance, SrF_2 and BaF_2 have better structural stability than CaF_2 under irradiation. When CaF_2 was irradiated with high energy alpha particles, point defects are mobile and either annihilate, aggregate, or become trapped, giving rise to color centers. Whereas color centers are not apparent in SrF_2 and BaF_2 because of the immobile defects on the cation sublattice.[26]

Therefore, it will greatly promote the development of solid-state nuclear laser spectroscopy and solid-state nuclear optical clocks if one kind of material can be found that ensures high VUV transmittance, high doping compatibility, low

luminescent noise and high radiation resistance stability.

3. Current solid-state nuclear clock materials

3.1. CaF_2 crystal

Thorium-doped calcium fluoride (Th:CaF_2) crystals are the most extensively studied solid-state nuclear clock material. They crystallize in the cubic fluorite structure, where Th^{4+} ions substitute for Ca^{2+} lattice sites, with charge compensation provided by double fluoride interstitials (F_i). Density functional theory (DFT) calculations indicate that this configuration generates a charge transfer state (CTS) near the band gap, potentially serving as an electron bridge channel for nuclear excitation.[25,27]

During 2022-2023, Kraemer *et al.* utilized CERN's ISOLDE facility to precisely measure the energy and lifetime of ^{229m}Th in CaF_2 and MgF_2 crystals.[21] Their results established the ^{229m}Th isomer energy at $\sim 8.338(24)$ eV, corresponding to an excitation wavelength of $\sim 148.71(42)$ nm. This work not only marked the first direct detection of ^{229m}Th decay signals but also reduced the uncertainty in the isomer energy by a factor of seven compared to previous reports.[28,29] In 2022, Beeks *et al.* from TU Wien developed a miniaturized crystal growth process, successfully producing ^{229}Th:CaF_2 crystals (Fig. 1, doping part Ø3.2×6 mm^3) with a ^{229}Th concentration of 10^{17} cm^{-3}.[16] These crystals with a thickness of 1 mm exhibited $\sim$ 35% transmittance near 149 nm, representing the highest performance reported for ^{229}Th-doped crystals at that time. The study also identified that radiation-induced dissociation and damage caused by ^{229}Th's intrinsic radioactivity severely degraded vacuum ultraviolet (VUV) transmittance. To maintain usable transparency, they recommended limiting the ^{229}Th doping concentration to less than 5×10^{17} cm^{-3}. However, subsequent research in 2024 by Beeks *et al.* demonstrated that annealing radiation-colored ^{229}Th:CaF_2 crystals in a carbon tetrafluoride (CF_4) atmosphere at 1250 °C effectively restored transparency and enhanced radiation resistance.[24]

Also in 2024, leveraging ^{229}Th:CaF_2 crystals from TU Wien, Tiedau *et al.* from the German National Metrology Institute (PTB) achieved the first successful direct laser excitation of the ^{229}Th nuclear transition in Th:CaF_2, marking a milestone in nuclear laser spectroscopy.[1] In the same year, Ye's group at the University of Colorado Boulder performed the first frequency comparison between the ^{229m}Th nuclear transition and an ^{87}Sr atomic clock within a ^{229}Th:CaF_2 crystal ($\nu_{Th}/\nu_{Sr} = 4.707072615078(5)$).[30] In 2025, Ye's group measured the temperature sensitivity of the ^{229}Th nuclear clock transition in CaF_2.[31] They observed a decrease in both the unsplit frequency and quadrupole splitting with increasing temperature. Notably, the $m = \pm 5/2 \rightarrow \pm 3/2$ transition exhibited the smallest temperature drift — merely 62(6) kHz over 143 K, equivalent to $\sim$ 0.4 kHz/K. Their analysis indicated that achieving 10^{-18} precision would require maintaining crystal temperature stability at $\sim$ 5 μK. While ^{229}Th:CaF_2 crystals offer significant advantages, including a wide bandgap, high thorium doping capacity, and an extended nuclear isomer lifetime, they face challenges: radiation damage induces F-center formation and Th^{3+} conversion, leading to drastic reductions in VUV transmittance. In 2024, Hiraki *et al.* from Okayama University and TU Wien demonstrated resonant x-ray pumping of the ^{229}Th isomer in a VUV-transparent ^{229}Th:CaF_2 crystal, measuring its radiative decay at 148.18 nm with a half-life of 447 s and discovering a controllable x-ray quenching effect for rapid isomer depletion.

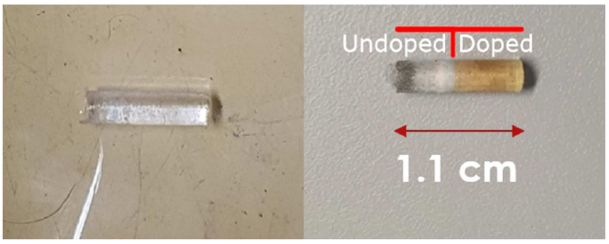


Fig. 1. The ^{229}Th:CaF_2 crystal grown at TU Wien.[16]

3.2. $LiSrAlF_6$ crystal

Thorium-doped lithium strontium aluminum fluoride ($LiSrAlF_6$, LiSAF) and lithium calcium aluminum fluoride ($LiCaAlF_6$, LiCAF) crystals were early research focal points. Both materials crystallize hexagonally, exhibit bandgaps exceeding 10 eV, and cover the 148.4 nm nuclear transition window. They share a similar structural framework composed of $[AlF_6]^{3-}$ octahedra, with Ca^{2+}/Sr^{2+} ions occupying octahedral lattice sites. Th^{4+} ions preferentially substitute into the size-matched Sr^{2+} or Ca^{2+} sites, with charge compensation via double fluoride interstitials (F_i). Theoretical calculations indicate that LiSAF possesses a lower doping formation energy than LiCAF due to its larger lattice volume.[32,33]

In 2015, the first optical-grade ^{229}Th:LiSAF crystal (Fig. 2) was successfully grown, with a ^{229}Th concentration of 10^{17} cm^{-3}.[15,34] Excitation of the nuclear transition was attempted using synchrotron radiation; however, no signals corresponding to the expected ^{229}Th nuclear transition (energy range 7.3–8.8 eV, lifetime range (1–2) s to (2000–5600) s) were detected. In 2024, a narrow-linewidth nuclear transition signal at 148.382 nm was observed for the first time in ^{229}Th:LiSAF under laser excitation, yielding a ^{229m}Th isomer energy of approximately 8.355733 eV in the LiSAF crystal.[2] ^{229}Th:LiSAF crystals are characterized by advantages including a wide bandgap, relatively high thorium doping compatibility, and chemical stability. However, significant challenges remain: (a) Compositional segregation is prone to occur during crystal growth; (b) Al^{3+} ions may be partially substituted

by Th^{4+} ions, leading to defect formation; (c) Th^{4+} ions can occupy multiple distinct lattice sites, resulting in inhomogeneous spectral broadening.

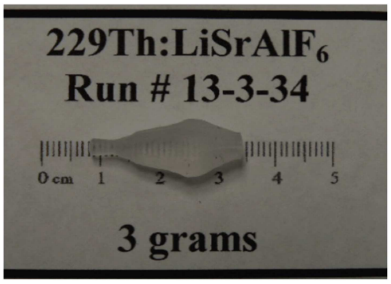


Fig. 2. The ^{229}Th:LiSAF crystal grown at the University of California, Los Angeles (UCLA), Oak Ridge National Laboratory (ORNL), and AC Materials Company.[33]

3.3. Novel fluoride crystals: LiF, $BaLiF_3$, and SrF_2

Significant progress has been made in ^{229}Th-doped crystal research; however, current material systems face substantial limitations. The variety of host matrices remains extremely limited, and primary candidate materials face challenges in co-optimizing key performance parameters. These constraints underscore the critical importance and urgency of developing novel thorium-doped crystalline materials. Nevertheless, research on new ^{229}Th-doped crystals is severely restricted by ^{229}Th's extreme scarcity, high toxicity, and intense radioactivity. Considering that ^{232}Th possesses identical electronic and chemical properties to ^{229}Th, alongside higher abundance, moderate toxicity, lower radioactivity, and easier handling, most current investigations into novel thorium-doped host crystals initially employ natural thorium (^{232}Th) as the dopant. This approach evaluates a material's feasibility and potential as a solid-state nuclear clock candidate.

During 2023–2025, a team led by Hang at the Shanghai Institute of Optics and Fine Mechanics (SIOM) conducted systematic theoretical and experimental investigations on three novel ^{232}Th-doped crystals (Th:LiF, Th:$BaLiF_3$, Th:SrF_2) and the prominent Th:CaF_2.[17–20] This work aimed to provide more viable and reliable material options for solid-state nuclear clock development, supporting high-precision nuclear timekeeping.

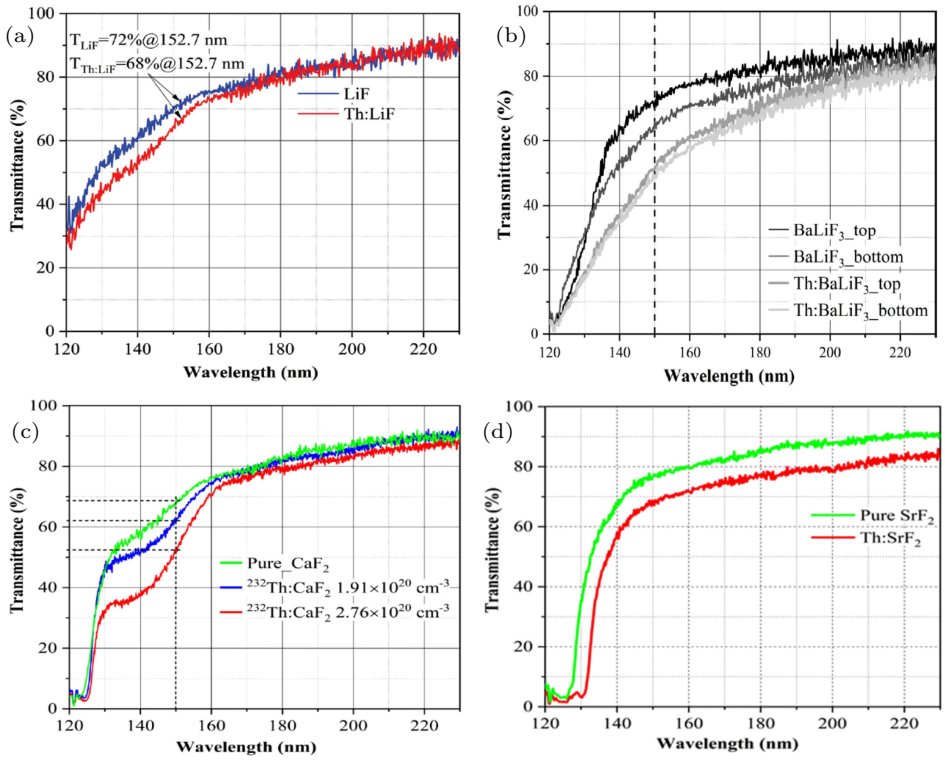


Fig. 3. VUV transmittance curves (120–230 nm) of the Th doped crystals with a thickness of 1 mm. (a) Th:LiF and LiF crystals, reproduced with permission from Ref. [17]; (b) $BaLiF_3$ and Th:$BaLiF_3$ crystals, reproduced with permission from Ref. [18]; (c) Th:CaF_2 and CaF_2 crystals, reproduced with permission from Ref. [19]; (d) SrF_2 and Th:SrF_2 crystals,[17–20] reproduced with permission from Ref. [20] ©Optical Society of America.

In 2023, ^{232}Th:LiF crystal was first reported.[17] Theoretical predictions suggested stabilization of Th^{4+} doping via Li vacancy compensation under fluorine-rich conditions. Experimentally, Th:LiF crystals demonstrated effective ^{232}Th doping ($\sim 10^{19}$ cm^{-3}) and excellent transmittance in the nuclear transition window ($> 65\%$ @150 nm for 1 mm thickness), only slightly lower than pure LiF crystals (Fig. 3(a)). The crystals also show promise for low background luminescence and radiation damage resistance.

In 2024, ^{232}Th:$BaLiF_3$ crystal was reported.[18] Theoretical predictions indicated stabilization of Th^{4+} doping through vacancy compensation mechanisms (e.g., Th substitution at Ba sites accompanied by Ba vacancies). Th:$BaLiF_3$ crystals were successfully grown, achieving effective ^{232}Th dop-

ing (3.13×10^{18} cm^{-3}). A transmittance of $\sim$ 50%@150 nm was measured for a 1 mm thick sample (Fig. 3(b)), identifying it as a potential candidate. However, the system's inherent Th^{4+} doping capacity is limited. Significant quantities of ThF_4 raw material are consumed and wasted to obtain usable doping levels. Given the current scarcity of ^{229}Th, research on ^{229}Th:$BaLiF_3$ crystals is not recommended.

Also in 2024, for the Th:CaF_2 system, preferred defect configurations were specified based on combined thermodynamic and kinetic factors, and their impact on VUV transmittance was evaluated.[19] Two highly doped ^{232}Th:CaF_2 crystals grown by the Czochralski method demonstrated excellent comprehensive performance, maintaining significant VUV transmittance at high doping concentrations. Transmittance values of $\sim$ 62% and $\sim$ 53% @150 nm for 1 mm thickness were achieved at doping concentrations of 1.91×10^{20} cm^{-3} and 2.76×10^{20} cm^{-3}, respectively (Fig. 3(c)). They exhibited only weak negative concentration dependence, significantly surpassing the performance of comparable high-concentration samples reported in the literature (e.g., $\sim$ 5% transmittance at 2.6×10^{20} cm^{-3} [13]).

In 2025, a novel candidate material for solid-state nuclear clocks, Th:SrF_2, was developed, showing significant application potential.[20] Compared to the segregation coefficients of other ^{232}Th-doped crystals (CaF_2: 0.3, LiF: 0.07), the segregation coefficient of 1.14 was achieved for ^{232}Th ions in SrF_2 crystal, indicating efficient incorporation of all Th from the feed material into the SrF_2 crystal without waste. This enables efficient, lossless utilization of Th, substantially reducing the difficulty of developing solid-state nuclear clock materials. ^{232}Th:SrF_2 crystals grown by the Czochralski method demonstrated excellent VUV transmittance ($\sim$ 69%@150 nm for 1 mm thickness) (Fig. 3(d)) alongside exceptionally high doping levels ($> 6 \times 10^{20}$ cm^{-3}). This highlights the superior tolerance of the SrF_2 lattice to Th ions and the significant potential of Th:SrF_2 as a solid-state nuclear clock material, positioning it as a prime candidate for future solid-state nuclear laser spectroscopy and clock research.

3.4. ThF_4 and ThO_2 films

Current ^{229}Th-doped crystals (e.g., CaF_2, LiSAF) face unavoidable challenges: the extreme scarcity and high radioactivity of ^{229}Th; the requirement for milligram-scale material during crystal growth, resulting in radioactivity levels $\geq$ 10 kBq and elevated safety risks; and significant processing difficulties, limiting the widespread adoption and integration of nuclear optical clocks. In contrast, thorium-doped thin films offer a novel pathway toward miniaturization and practical application due to their low material consumption and compatibility with semiconductor processing techniques.

In 2019, Gouder reported a ThF_4 bandgap of $\sim$ 10 eV, indicating its suitability as a nuclear clock material.[35] In 2024, Osipenko conducted a quantitative study of ThF_4 thin film luminescence properties.[36] Ultraviolet photoluminescence and radioluminescence were measured for the first time in ThF_4 films, demonstrating signal levels comparable to PMT dark counts and thus not interfering with ^{229m}Th signal detection, further confirming the feasibility of ThF_4 films for nuclear clocks. In the same year, microgram-scale ^{229}Th material was used to prepare ThF_4 thin films (thickness 30–100 nm, diameter 50 μm–5 mm) via a miniaturized physical vapor deposition (PVD) technique (Fig. 4).[22] Radioactivity was reduced by three orders of magnitude compared to conventional doped crystals, effectively overcoming challenges posed by ^{229}Th scarcity and radiological handling. Crucially, direct laser excitation of the nuclear clock transition was achieved for the first time in ThF_4 films, with the transition frequency determined, laying the groundwork for integrated nuclear clocks.

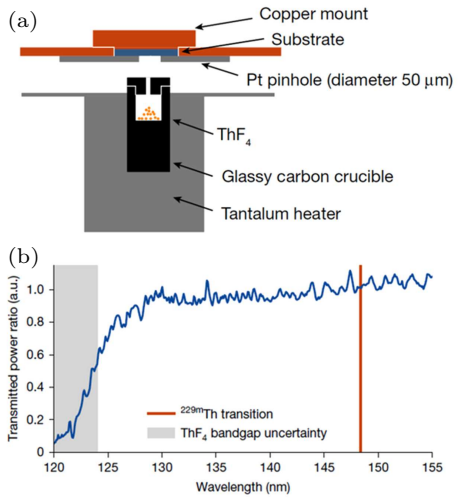


Fig. 4. The $^{229}ThF_4$ target fabrication procedure and characterization. (a) Schematic of the $^{229}ThF_4$ target vapor deposition setup; (b) VUV transmission of a similarly fabricated ThF_4 thin film of about 1 μm thickness. Reproduced with permission from Ref. [22].

ThO_2 thin films represent another candidate material. Although ThO_2 possesses a lower bandgap ($\sim$ 6 eV), nuclear transitions were detected within opaque ThO_2 films via conversion electron Mössbauer spectroscopy (CEMS) in 2025.[23] This expanded the range of viable thin-film material choices, particularly suitable for non-optical detection schemes. And they demonstrated superior high-temperature stability compared to fluoride materials.

ThF_4 and ThO_2 thin films, as nuclear clock materials, offer the paramount advantage of reducing ^{229}Th consumption to the microgram-scale, drastically diminishing radioactivity. The thin-film format simultaneously enables high particle density and miniaturization prospects. However, a fundamental drawback and significant challenge is the extreme difficulty in achieving high-quality single-crystalline thin film growth.

Furthermore, substrate interference is difficult to avoid, and effective strategies to suppress the inevitable inhomogeneous broadening within the films must be developed.

Table 1. Comparison of Th doping concentration and VUV transmittance of the doped crystals.

Crystals	VUV transmittance	Th concentration (cm^{-3})	Ref.
^{229}Th:CaF_2	~ 35%@149 nm	$\sim 10^{17}$	[13]
^{229}Th:LiSAF	–	$\sim 10^{17}$	[15]
^{232}Th:LiF	~ 66%@150 nm	$\sim 8.23\times10^{18}$	[17]
^{232}Th:$BaLiF_3$	~ 50%@150 nm	$\sim 3.28\times10^{18}$	[18]
^{232}Th:CaF_2	~ 53%@150 nm	$\sim 2.75\times10^{20}$	[19]
^{232}Th:CaF_2	~ 5%@150 nm	$\sim 2.60\times10^{20}$	[16]
^{232}Th:SrF_2	~ 69%@150 nm	$\sim 6.29\times10^{20}$	[20]

In summary, Th-based or Th-doped VUV materials reported experimentally and theoretically for solid-state nuclear clock applications primarily include crystals such as CaF_2, MgF_2, LiSAF, LiF, $BaLiF_3$, SrF_2, alongside thin films including ThF_4 and ThO_2. Among these, only LiSAF, MgF_2, and CaF_2 crystals, as well as ThF_4 and ThO_2 thin films, have employed ^{229}Th for nuclear precision spectroscopy experiments. Decay signals from ^{229m}Th de-excitation were first directly detected in ^{229m}Th-implanted MgF_2 and CaF_2 crystals, concurrently reducing nuclear transition energy uncertainty by approximately an order of magnitude. Subsequently, direct laser excitation of the nuclear transition was successfully achieved in ^{229}Th:CaF_2 crystal, ^{229}Th:LiSAF crystal, $^{229}ThF_4$, and $^{229}ThO_2$ thin films. Collectively, these results demonstrate the considerable promise and inherent advantages of the solid-state approach for nuclear optical clock research. Furthermore, Th:SrF_2 crystals exhibit exceptional VUV transmittance and extremely high doping levels, strongly highlighting the significant potential of the SrF_2 host as a solid-state nuclear clock material. Consequently, this system is anticipated to serve as a prime candidate for future solid-state nuclear laser spectroscopy and clock development.

4. Defects in solid-state nuclear clock materials

Defects are one of the most significant factors affecting the transmittance of Th-doped crystals at ~ 148 nm. Defects can be divided into inherent defects and defects caused by irradiation. Under different types of irradiations, the internal defects of crystals differ, thereby variably affecting the performance of crystals. Under VUV irradiation, crystals doped with Th^{4+} typically produce point defects caused by electroneutral equilibrium. Point defects refer to defects in the crystal lattice with the size of an atom, which can generally be divided into Frenkel and Schottky defect systems. In Schottky defect systems, the crystal structure is closely packed, so there are no interstitial atoms, only vacancies as defects. Defect charge compensation is achieved through vacancies with the same number of cations or anions. In electrically neutral crystals, vacancies are not required to be charge-compensated. In Frenkel defect systems, vacancies and interstitial atoms of the same type coexist. While these crystals have band gaps of > 10 eV, impurities and color centers can cause residual absorption and may interfere with the ^{229}Th optical spectroscopy. Various metal ions as well as oxygen-based impurities at the part-per-million level can lead to absorption coefficients of up to 0.1 cm^{-1}.[37] To ensure crystal transparency, standard purification methods can be employed to reduce these impurities to part-per-billion levels. For the development of solid-state nuclear optical clocks, exploring more solid-state nuclear optical clock materials with application potential and studying their defect properties is crucial to understanding the internal dynamics of crystals.

First-principles methods based on density functional theory have been widely proven to be an effective way to study crystal material doping, structure, defects, physical and chemical properties, and their microscopic mechanisms. On the one hand, using DFT to construct potential Th-containing complex defect models allows for the investigation of their defect formation energies and the resulting impacts on the crystal structure. This enables a comprehensive assessment, from both thermodynamic and kinetic perspectives, on whether Th-related defects can readily form in the crystal to achieve effective doping. On the other hand, by employing hybrid functionals (such as HSE06, HSE03, PBE0, etc.[38–41]) to calculate the electronic structure of crystal models containing Th-related defects, the energy levels and orbital compositions of the defects introduced by doping can be determined. By comparing the bandgap with the nuclear transition energy, the influence of Th doping on the material's transmittance performance in the nuclear transition wavelength range can be evaluated.

In 2009, Jackson *et al.*[31] studied the doping sites of Th ions and the corresponding charge compensation mechanisms in Th-doped $LiCaAlF_6$ and $LiSrAlF_6$ crystals through theoretical calculations, and anticipated their prospects as solid-state nuclear clocks. In 2010, Rellergert *et al.*[32] conducted a detailed theoretical analysis of the concept of driving nuclear transitions in crystals to establish a solid-state optical frequency standard, investigating the effects of the crystal environment on nuclear transitions and the performance of solid-state nuclear optical clocks, and initially assessing the precision ($\sim 10^{-16}$) and stability ($\sim 10^{-17}$–10^{-15}) that solid-state nuclear optical clocks could achieve, demonstrating the unique potential of solid-state nuclear optical clocks in limiting the time variation of fundamental constants. In 2018, Nickerson *et al.*[42] theoretically investigated the collective effects in Th:CaF_2 crystals on laser-driven nuclear transitions. Their study considered the influence of potential doping sites, quantized axis orientations, and laser pulse configurations on both the intensity of scattered light and the characteristics of nu-

clear excitation. The theoretical findings support the experimental feasibility of using coherent laser radiation to directly drive nuclear transitions. In 2020, Pimon *et al.*[43] investigated Th:MgF_2 crystals through theoretical calculations, evaluating the doping potential of Th, the charge compensation mechanisms introduced by doping, and changes in crystal structure and bandgap. The results indicated that MgF_2 crystals are not suitable as solid-state nuclear optical clock materials. In the same year, Nickerson *et al.*[11] theoretically studied the concept of using defect energy levels in Th-doped crystals as electronic bridges to indirectly excite nuclear transitions, using Th:CaF_2 crystals as an example. The study concluded that this indirect approach could increase the probability of exciting the nuclear transition by at least two orders of magnitude compared to the direct laser excitation scheme. It was also noted that the reverse process of the electronic bridge similarly enhances the decay process of the isomeric state. In 2021, Nickerson *et al.*[26] conducted a further theoretical investigation into the potential electronic bridge processes in Th-doped crystals, exploring the dominant coupling mechanisms involved in such processes. It was highlighted that the reverse electronic bridge process could enhance the performance of nuclear clocks. In 2022, Pimon *et al.*[44] conducted theoretical calculations on the bandgap of Th:LiCAF crystals and found that the bandgap of Th:LiCAF is significantly greater than the energy of the isostructural states of ^{229}Th, thus allowing the crystal to remain transparent within the nuclear transition wavelength range. This indicates that Th:LiCAF possesses potential as a material for solid-state nuclear optical clocks. Also in 2022, Beeks *et al.*[25] from the TU Wien employed the temperature gradient technique to grow Th-doped CaF_2 crystals and investigated their defect structures. Fluorine deficiency during the growth process led to the formation of metallic calcium clusters, which were partially remedied through annealing treatment. DFT calculations revealed that a charge compensation mechanism mediated by interstitial F ions oriented at 90° to each other is the most probable configuration. After doping with Th^{4+} ions, the structure of the cation and anion clusters transformed from a cube to a square antiprism, and it is pointed that defects exhibit absorption in the VUV band of the crystal. $^{229}Th^{4+}$ ions are expected to substitute at the Ca^{2+} location in LiCAF along with two F interstitials for charge compensation.[45]

In 2023, Hang's group at SIOM reported the Th:LiF single crystal. Through DFT predictions and testing of the grown crystals, it was found that thorium ions can be doped effectively by the energetically favorable charge compensation mechanisms without obvious negative effect on the transmittance of Th:LiF crystal in the nuclear transition band in an F-rich environment.[17] In 2024, they successfully grew Th:$BaLiF_3$ single crystals and combined the charge compensation mechanism designed by DFT calculations. It was found that the Th-5f and 6d defect energy levels introduced by Th doping at the bottom of the conduction band slightly reduced the band gap from 9.037 eV to 8.950 eV, causing a slight red shift in the VUV cutoff edge. The theoretical research results support that Th:$BaLiF_3$ crystal can achieve effective doping of Th ions and remain transparent in the nuclear transition band, and can be further studied as a candidate for solid-state nuclear optical clock material.[18] In the same year, Hang's group also investigated the defect configurations in Th:CaF_2. Based on kinetic and thermodynamic stability analyses, they determined that the F interstitial configuration is the most probable. Calculations further revealed that the band gap of the Th-containing defect structure is slightly reduced to 9.318 eV, which remains significantly higher than the nuclear transition energy. Consequently, the VUV transmittance of the doped crystal is only marginally lower than that of pure CaF_2.[19] In 2025, they reported the crystal growth of Th:SrF_2, and calculated that F-gap defect configurations were more likely to exist and analyzed the defect energy levels in PDOS and found that the introduction of Th-6d energy levels slightly reduced the bandgap width, causing a red shift in the VUV cutoff edge.[20] No significant color centers were formed in SrF_2 after α irradiation, indicating its excellent radiation stability.[26] In 2025, researchers at Okayama University utilized synchrotron radiation to investigate defects in Th:CaF_2 crystals.[46] They proposed that x-ray induced ^{229m}Th quenching in CaF_2 is related to defect levels of thorium dopants and crystal host.

5. Effects of crystal environment on ^{229}Th nuclear transitions

5.1. Effects of crystal environment on ^{229}Th nuclear energy levels

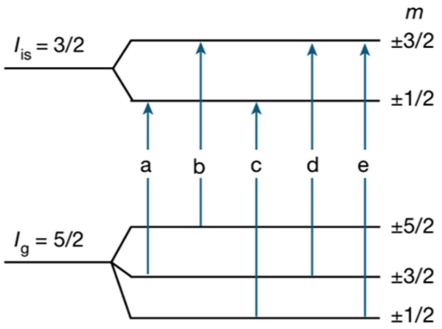
At a time when the absolute transition frequency of the ^{229}Th nuclear in crystals was not determined experimentally by direct laser excitation, researchers have estimated the frequency shift and broadening of ^{229}Th nuclear transitions. ^{229}Th atoms in a solid-state crystal lattice are confined in the Lamb–Dicke regime, i.e., the recoil energy $E_{\text{recoil}} = (8.4\ \text{eV})^2/(2M_{\text{Th}}c^2) \approx 1.6 \times 10^{-10}$ eV is much less than the energy required to create a phonon in the lattice, so the internal and external degrees of freedom are decoupled.[32,47] As a result, the transition of $^{229m}\text{Th} \rightarrow {}^{229g}\text{Th}$ is not sensitive to recoil or first order Doppler effects. However, the nuclear transition is affected by the interaction between the crystal lattice environment and the ^{229}Th nuclear levels, causing some effects such as energy level splitting, shifting, and inhomogeneous broadening. In a crystal without external fields, the Hamiltonian for a ^{229}Th nucleus can be written as $H = H + H_{\text{FS}} + H_{\text{HFS}}$, where H is the single-particle nuclear Hamiltonian,

H_{FS} and H_{HFS} are the fine and hyperfine interactions, respectively, describing the effects between ^{229}Th nucleus and crystal environment.[32] There are no unpaired electrons in ionically bonded crystals such as ^{229}Th:CaF_2, ^{229}Th:$LiSrAlF_6$, $^{229}ThF_4$ and $^{229}ThO_2$. Therefore, the fine-structure interaction (H_{FS}) of the ^{229}Th nuclei with the crystal lattice environment is absent. The dominant source of shifts and broadenings of the ^{229}Th nuclear transition comes from the hyperfine interactions. The hyperfine Hamiltonian can be written in a multipole expansion $H_{FS} = H_{E0} + H_{M1} + H_{E2} + \cdots$, where H_{E0}, H_{M1} and H_{E2} are the electric monopole, the magnetic dipole, and the electric quadrupole terms, respectively.[9,32]

The electric monopole term (H_{E0}) describes the contact interaction between the electron cloud and the nucleus, leading to a shift of the nuclear transition. Since the electron cloud density is temperature dependent, the temperature fluctuation and gradients across the ^{229}Th doped crystal will cause inhomogeneous line broadening. The shift is 0.1–1 GHz compared to free ions, and the temperature dependence of the shift is estimated as ~ 10 kHz/K.[9,32,48,49] The magnetic dipole interaction term (H_{M1}) describes the interaction between the ^{229}Th nucleus and the magnetic fields of surrounding nuclei. It contributes to inhomogeneous broadening and is temperature independent. The corresponding broadening was estimated to be 1–10 kHz in Ref. [32] and to $2\pi\cdot$(84–251) Hz in Ref. [9].

The electric quadrupole term (H_{E2}) describes the interaction between the electric quadrupole moment of the ^{229}Th nucleus and the electric field gradient at the position of the nucleus. It gives rise to a shift and splitting in the transition energy. The electric field gradient at the position of the ^{229}Th nucleus is zero in cubic crystal $^{229}ThO_2$, while it is non-vanishing in monoclinic crystal $^{229}ThF_4$ and even in ^{229}Th doped cubic crystal (e.g., CaF_2) because of charge compensation defects.[9,22,50] The transition energy shifts will be 1 kHz–100 MHz under a typical electric field gradient of 10^{16}–10^{21} V/m^2.[32,51,52] The quadrupole splitting in ^{229}Th:CaF_2 crystal was estimated to be a few hundreds of MHz.[9] The vibration of the nuclei leads to second order Doppler effects, which can cause a shift about $2\pi \cdot 1.14 \cdot T$ (in Hz) and broadening of about $2\pi \cdot 0.93 \cdot T$ (in Hz), where T is the temperature in Kelvins.[9] It is noteworthy that the electric monopole term, the electric quadrupole term, and the second-order Doppler effect are temperature dependent. As temperature control technology advances, the shift and broadening of ^{229}Th nuclear transitions will be better controlled.

In 2024, the research group led by Ye measured the nuclear quadrupole structure of the ^{229}Th nuclear transition in CaF_2 150(1) K with a VUV optical frequency comb system for the first time.[29] The electric field gradient at the position of the ^{229}Th nucleus is produced by the surrounding lattice ions and F^- interstitials, leading to the splitting of ground state and isomeric excited state (Fig. 5). They determined the absolute frequencies and assigned to the corresponding sublevel transitions (Fig. 5). Then, they fitted the measured line centres to the predicted quadrupole structure, yielding an electric field gradient of 109.1(7) V·Å^{-2} for the ^{229}Th:CaF_2 crystal.



m_g	m_{is}	ν_{Th} (MHz)
3/2	1/2	2,020,407,283.847(4)
5/2	3/2	2,020,407,298.727(4)
1/2	1/2	2,020,407,446.895(4)
3/2	3/2	2,020,407,530.918(4)
1/2	3/2	2,020,407,693.98(2)

Fig. 5. The nuclear level diagram of ^{229}Th in CaF_2 at 150(1) K and the absolutely frequencies assigned to their corresponding sublevel transitions. Reproduced with permission from Ref. [29].

In the same year, Ye's group performed DFT calculations using the monoclinic crystal structure of $^{229}ThF_4$.[22] ^{229}Th atoms have two non-equivalent sites in $^{229}ThF_4$ crystal (Fig. 6(a)). They experience different crystal electric field gradients of 310.5 V·Å^{-2} and 308.9 V·Å^{-2}, respectively, leading to non-degenerate nuclear energy levels and distinct laser spectra (Fig. 6(b)). They pointed out that the magnetic dipole–dipole interaction between the ^{229}Th nuclei and the nearby ^{19}F nuclei is the main source of inhomogeneous broadening of the nuclear clock transitions. The magnetic field seen by a thorium nucleus was estimate to fluctuate with a standard deviation of approximately 5 G, resulting in Zeeman-limited linewidths of 1–7 kHz for the various transitions. The least broadening is about 1.1 kHz, corresponding to the $5/2, \pm 1/2\rangle \leftrightarrow 3/2, \mp 1/2\rangle$ transition for type 2 sites (Fig. 6(b)).

In 2025, Ye's group reported on the temperature sensitivity of ^{229}Th nuclear transition in CaF_2.[30] They measured the four strongest transitions at 150 K, 229 K, and 293 K, and observed shifts of the unsplit frequency and the electric quadrupole splittings. On the one hand, when the temperature of ^{229}Th:CaF_2 increases, the crystal lattice expansion and thermal population of higher energy phonon modes will decrease the electron density at the nucleus, inducing an isomeric shift of all lines and a decrease of unsplit frequency. On the other hand, the electric field gradient and its asymmetry decrease with temperature increase, reducing the quadrupole splitting. They observed that, among the four lines, the $m = \pm 5/2 \rightarrow \pm 3/2$ transition is much less sensitive to temperature change

(62(6) kHz over 143 K range) due to a fortuitous partial cancellation of the isomeric shift and splitting.

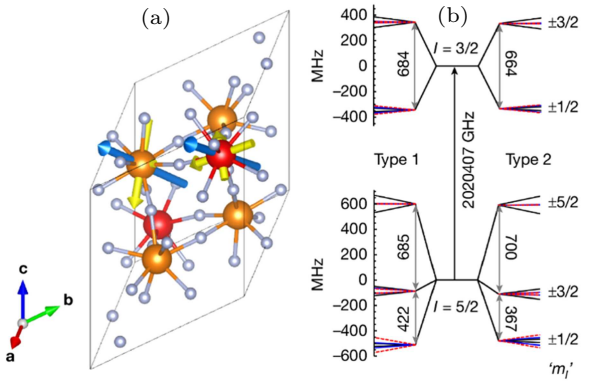


Fig. 6. (a) Unit cell of $^{229}ThF_4$ showing the crystal electric field eigenvectors. Thorium atoms are shown as red and orange spheres, and fluorine atoms are shown in grey. The vectors show the diagonal crystal electric field components. (b) Numerically calculated crystal electric field and Zeeman splittings in the two inequivalent thorium sites. Reproduced with permission from Ref. [22].

In the same year, they further observed a zero-shift temperature where the local slope of the $m = \pm 5/2 \rightarrow \pm 3/2$ transition frequency versus temperature curve vanishes at 195(5) K.[53] They also found that lower ^{229}Th doping concentration leads to a narrower transition linewidth, and observed much larger linewidths of 10 s to 100 s of kHz in CaF_2 than those of previous estimations.[9] They suggested that each ^{229}Th dopant distorts the CaF_2 lattice and creates a long-range microstrain extending over many lattice spacings. These defects are randomly dispersed throughout the crystal, and lead to different electric field gradients and electron densities at the ^{229}Th nucleus sites, resulting in different nuclear transition splitting and shifting. This could be the main inhomogeneous broadening mechanism in ^{229}Th:CaF_2.

In 2025, Hudson's group evaluated the ^{229}Th isomer shifts in $LiSrAlF_6$, CaF_2, ThF_4, $BaMgF_4$ and $BaZnF_4$ via combining relativistic many-body methods of atomic structure with periodic density functional theory.[54] They reported the isomer shift for different sites in these crystals. For example, the isomer shift between the two nonequivalent sites is 4(1) MHz in $^{229}ThF_4$, while the shift between the two doping sites (F-90°-F and F-180°-F) in CaF_2 is 14(4) MHz. They predicted that the nuclear clock frequencies for these crystals equal 2020407384(40) MHz. It constrains the nuclear transition frequencies to a window of 80 MHz. In the same year, they reported on the laser-based conversion electron Mössbauer spectroscopy of $^{229}ThO_2$.[23] In $^{229}ThO_2$, the excited nucleus quickly decays by internal conversion because the band gap ($\sim$ 6 eV) of ThO_2 is smaller than the nuclear isomeric state energy (8.4 eV). They determined the ^{229}Th nuclear transition frequency experimentally and calculated the isomer shift theoretically. An isomer shift of $\sim$ 100 MHz between bulk $^{229}ThO_2$ and ^{229}Th:$LiSrAlF_6$ is expected.

In the same year, they proposed a new crystal $^{232}Th(SO_4)_2$ for a high-performance solid-state ^{229}Th nuclear clock.[55] Using state-of-the-art calculations, they found that this crystal has a large band gap ($\sim$ 9 eV), and, what's more important, is a nuclear spin free material. Its spinless characteristic would cancel the nuclear line broadening caused by the nuclear magnetic dipole–dipole interaction, and enable a solid-state nuclear clock with low instability.

5.2. Effects of crystal environment on ^{229}Th radiative decay rate

In solid materials, the radiative decay rate of the ^{229}Th nuclear clock isomer can be affected by multiple factors such as crystal environment, potential defect states, and internal conversion process. As shown in Table 2, the radiative decay lifetimes of ^{229m}Th in different crystals vary and are much shorter than that in an ion trap. The ^{229m}Th isomer mainly decays to the ground state by magnetic-dipole radiation, corresponding to a vacuum isomer lifetime of 1900–2500 s.[1,2,7,21] However, when a ^{229}Th atom is embedded into a transparent non-magnetic dielectric medium with refractive index n, the magnetic-dipole decay rate is increased by a factor of n^3 compared with its vacuum value because of photon mode field renormalization and the change in the photon density of states.[56–58] Apart from this effect, the decay rate can also be modified by new competing non-radiative decay channels.

Table 2. The radiative decay lifetimes of ^{229m}Th in different systems.

Systems	Population way of ^{229m}Th	Lifetime (s)	Ref.
$^{229}Th^{3+}$ in ion trap	α decay of ^{233}U	2020^{+866}_{-433} [a)]	[7]
^{229}Th:MgF_2	β decay of ^{229}Ac	967(147)[b)]	[21]
^{229}Th:CaF_2	laser excitation	630(15)	[1]
^{229}Th:CaF_2	laser excitation	641(4)	[29]
^{229}Th:CaF_2	x-ray excitation	645(36)[c)]	[59]
^{229}Th:$LiSrAlF_6$	laser excitation	$568(13)_{stat}(20)_{sys}$	[2]
^{229}Th:F_4 film on Al_2O_3	laser excitation	$150(15)_{stat}(5)_{sys}$	[22]
^{229}Th:F_4 film on MgF_2	laser excitation	$153(9)_{stat}(7)_{sys}$	[22]
^{229}Th:O_2	laser excitation	0.0123(3)	[23]

[a)] The radiative decay half-life is 1400^{+600}_{-300} s; [b)] the radiative decay half-life is 670(102) s;
[c)] the radiative decay half-life is 447(25) s.

In 2024, Hiraki *et al.* observed a ∼ 10 times shorter isomer decay lifetime in ^{229}Th:CaF_2 crystal during x-ray beam irradiation at room temperature, and suggested the existence of additional decay paths.[60] Subsequently, laser-induced quenching of the ^{229}Th isomer was observed in both ^{229}Th:$LiSrAlF_6$ and ^{229}Th:CaF_2 crystals.[60,61] In 2025, Guan *et al.* further investigated the x-ray-induced quenching experimentally and proposed a mechanism.[46] As shown in Fig. 7, electrons trapped in crystal defects can be activated by x-ray or laser stimulation, then they migrate and are captured in the intermediate state at the ^{229}Th dopant. One ^{229m}Th can decay by transferring its energy to a trapped electron at an intermediate level (an internal conversion process), and isomer quenching takes place.

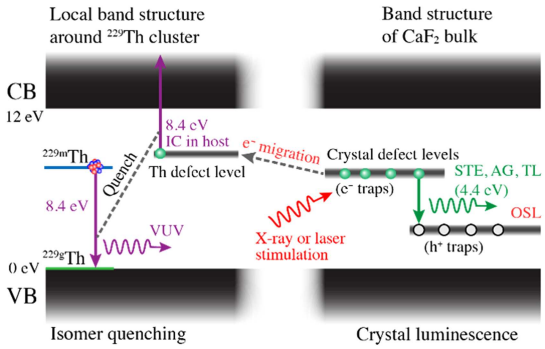


Fig. 7. Conceptual band structure of the Th:CaF_2. Reproduced with permission from Ref. [46].

In 2024, Ye's group reported on the lifetimes of the isomeric transition of ^{229}ThF_4 film on Al_2O_3 and MgF_2, which are markedly shorter than the value in ^{229}Th:CaF_2 and ^{229}Th:$LiSrAlF_6$.[22] They concluded that the shorter isomer lifetime could arise from some other potential quenching effects besides a high refractive index of ^{229}ThF_4. The nuclear degree of freedom and mixed-parity electronic states by the crystal fields are coupled by hyperfine interaction. It will enable a new electric-dipole decay channel for the isomeric state. The quenching effects could also arise from the amorphous structure of the film, bulk and surface impurities and stray surface charges.

In 2025, Hudson's group excited the nuclear transition in a thin ^{229}ThO_2 film.[23] The ^{229m}Th isomer will quickly decay by internal conversion and result in ejection of electrons from the surface because the band gap of ThO_2 (∼ 6 eV) is considerably smaller than the isomeric energy (8.4 eV). This internal conversion process can reduce the isomeric state lifetime to only ∼ 10 μs, and it is sensitive to the local crystal lattice environment.

6. Perspective and outlook

The transition from the exceptionally low-energy and long-lived excited state (isomer) of the isotope ^{229}Th is expected to be less susceptible to environmental perturbations than electronic transition. It enables a solid-state clock based on ^{229}Th embedded solid materials. Solid-state clocks could be exceptionally stable and compact due to a large number of ^{229}Th nuclei and a small core physical component. The essential requirements for candidate ^{229}Th host material are high doping efficiency, high optical transmittance at ∼ 148 nm, and high radiation damage resistance. ^{229}Th doped or ^{229}Th-based solid materials have played a crucial role in the development of nuclear optical clocks. For example, the world's first observation of the luminescence from ^{229m}Th nuclear transitions and the first laser excitation and precise measurement of nuclear transition frequencies were both carried out ^{229}Th based solid materials.

There are various defects in Th-doped crystal materials, and the possible sources include: (1) differences in radius and valence state between Th^{4+} ions and substituted metal cations; (2) point defects, dislocations, and grain boundaries generated during material fabrication; (3) damage to the lattice structure caused by high-energy rays produced by ^{229}Th nuclear decay and VUV laser irradiation. These defects will have adverse effects on the optical transmittance, background luminescence noise, and damage resistance of the crystal. In the future, the preparation of ^{229}Th-doped crystals and stoichiometric ^{229}Th fluorides needs to minimize the formation of these defects.

The ^{229}Th nuclear transition is affected by the interaction between crystal lattice environment and the ^{229}Th nuclear levels, leading to energy level splitting, shifting, inhomogeneous broadening, and quenching. The crystal lattice environment can be affected by defects, strains, impurities, space charge, temperature fluctuations, etc. Part of the physical mechanisms behind these influences are not yet fully understood, requiring more in-depth research. It is necessary to improve the quality of current ^{229}Th based solid materials, reducing defects, minimizing the inhomogeneous broadening of nuclear transition energy levels. In the future, there is a need to develop new solid-state materials with excellent comprehensive performance, and advance toward miniaturization and integration such as thin films and waveguides.

Acknowledgements

This work was supported by Zhangjiang Laboratory (Grant No. ZJSP21A001D), the Strategic Priority Research Program of the Chinese Academy of Sciences (Grant No. XDB0920000), and the National Natural Science Foundation of China (Grant Nos. 12341402 and 12341403).

References

[1] Tiedau J, Okhapkin M V, Zhang K, Thielking J, Zitzer G, Peik E and Schumm T 2024 *Phys. Rev. Lett.* **132** 182501

[2] Elwell R, Schneider C, Jeet J, Terhune J, Morgan H, Alexandrova A, Tran Tan H, Derevianko A and Hudson E 2024 *Phys. Rev. Lett.* **133** 013201

[3] Peik E and Tamm C 2003 *Europhys. Lett.* **61** 181

[4] Peik E, Zimmermann K, Okhapkin M and Tamm C 2009 *Frequency Standards and Metrology* 532

[5] Campbell C J, Radnaev A G, Kuzmich A, Dzuba V, Flambaum V and Derevianko A 2012 *Phys. Rev. Lett.* **108** 120802

[6] Peik E, Schumm T, Safronova M S, Pálffy A, Weitenberg J and Thirolf P G 2021 *Quantum Sci. Technol.* **6** 034002

[7] Yamaguchi A, Shigekawa Y, Haba H, Kikunaga H, Shirasaki K, Wada M and Katori H 2024 *Nature* **629** 62

[8] Rellergert W G, Sullivan S T, DeMille D, Greco R R, Hehlen M P, Jackson R A, Torgerson J R and Hudson E R 2010 *IOP Conf. Ser: Mater. Sci. Eng.* **15** 012005

[9] Kazakov G A, Litvinov A N, Romanenko V I, Yatsenko L P, Romanenko A V, Schreitl M, Winkler G and Schumm T 2012 *New J. Phys.* **14** 083019

[10] Itano W M, Bergquist J C, Bollinger J J, Gilligan J M, Heinzen D J, Moore F L, Raizen M G and Wineland D J 1993 *Phys. Rev. A* **47** 3554

[11] Nickerson B S, Pimon M, Bilous P V, Gugler J, Beeks K, Sikorsky T, Mohn P, Schumm T and Pálffy A 2020 *Phys. Rev. Lett.* **125** 032501

[12] L von der Wense L and Seiferle B 2020 *Eur. Phys. J. A* **56** 277

[13] Beeks K, Sikorsky T, Schumm T, Thielking J, Okhapkin M and Peik E 2021 *Nat. Rev. Phys.* **3** 238

[14] Alvarez R 2013 *Sci. Glob. Secur.* **21** 53

[15] Jeet J, Schneider C, Sullivan S T, Rellergert W, Mirzadeh S, Cassanho A, Jenssen H, Tkalya E and Hudson E 2015 *Phys. Rev. Lett.* **114** 253001

[16] Beeks K, Sikorsky T, Rosecker V, Pressler M, Schaden F, Werban D, Hosseini N, Rudischer L, Schneider F, Berwian P, Friedrich J, Hainz D, Welch J, Sterba J H, Kazakov G and Schumm T 2023 *Sci. Rep.* **13** 3897

[17] Gong Q, Zhao C, Tao S, Hang Y, Zhu S and Ma L 2023 *Adv. Opt. Mater.* **11** 2202327

[18] Gong Q, Tao S L, Li S, Deng G, Zhao C and Hang Y 2024 *Phys. Rev. A* **109** 033109

[19] Gong Q, Tao S, Zhao C, Hang Y, Zhu S and Ma L 2024 *Inorg. Chem.* **63** 3807

[20] Gong Q, Li L, Li S, Zhang S, Tao S, Deng G, Zhang P, Zhao C, Hang Y, Zhu S and Ma L 2025 *Opt. Lett.* **50** 2290

[21] Kraemer S, Moens J, Athanasakis-Kaklamanakis M, Bara S, Beeks K, Chhetri P, Chrysalidis K, Claessens A, Cocolios T E, Correia J G M, Witte H D, Ferrer R, Geldhof S, Heinke R, Hosseini N, Huyse M, Köster U, Kudryavtsev Y, Laatiaoui M, Lica R, Magchiels G, Manea V, Merckling C, Pereira L M C, Raeder S, Schumm T, Sels S, Thirolf P G, Tunhuma S M, Van Den Bergh P, Van Duppen P, Vantomme A, Verlinde M, Villarreal R and Wahl U 2023 *Nature* **617** 706

[22] Zhang C, von der Wense L, Doyle J F, Higgins J S, Ooi T, Friebel U U, Ye J, Elwell R, Terhune J, Morgan H, Alexandrova A, Tran Tan H, Derevianko A and Hudson E R 2024 *Nature* **636** 603

[23] Elwell R, Terhune J E S, Schneider C, Morgan W T, Tran Tan H B, Perera U C, Rehn D A, Alfonso M C, von der Wense L, Seiferle B, Scharl K, Thirolf P G, Derevianko A and Hudson E R 2025 arXiv:2506.03018

[24] Beeks K, Sikorsky T, Schaden F, Pressler M, Schneider F, Koch B N and Schumm T 2024 *Phys. Rev. B* **109** 094111

[25] Beeks K 2022 *The Nuclear Excitation of Thorium-229 in the CaF_2 Environment* (Ph.D. Dissertation) (Vienna: Vienna University of Technology)

[26] Weber W J 1983 *Radiation Effects* **70** 217

[27] Nickerson B S, Pimon M, Bilous P V, Gugler J, Kazakov G A, Sikorsky T, Beeks K and Grüneis A 2021 *Phys. Rev. A* **103** 053120

[28] Seiferle B, von der Wense L, Bilous P V, Amersdorffer I, Lemell C, Libisch F, Stellmer S, Schumm T, Düllmann C E, Pálffy A and Thirolf P 2019 *Nature* **573** 243

[29] Sikorsky T, Geist T, Hengstler D, Kempf S, Gastaldo L, Enss C, Mokry C, Runke J and Düllmann C E 2020 *Phys. Rev. Lett.* **125** 142503

[30] Zhang C, Ooi T, Jacob S, Kempf S, Gastaldo L, Enss C, Mokry C, Runke J and Düllmann C E 2024 *Nature* **633** 63

[31] Higgins J S, Ooi T, Doyle J F, Zhang C, and Ye J, Beeks K, Sikorsky T and Schumm T 2025 *Phys. Rev. Lett.* **134** 113801

[32] Jackson R A, Amaral J B, Valerio M E G, DeMille P and Hudson E R 2009 *J. Phys.: Condens. Matter* **21** 325403

[33] Rellergert W G, DeMille D, Greco R, Hehlen M P, Torgerson J R and Hudson E R 2010 *Phys. Rev. Lett.* **104** 200802

[34] Jeet J 2018 *Search for the low lying transition in the ^{229}Th nucleus* (Ph.D. Dissertation) (Los Angeles: University of California, Los Angeles)

[35] Gouder T, Eloirdi R, Martin R L, Osipenko M, Giovannini M and Caciuffo R 2019 *Phys. Rev. Research* **1** 033005

[36] Osipenko M, Carrapico C, Burdeinyi D, Caciuffo R, Eloirdi R, Giovannini M, Kellerbauer A, Malmbeck R, Ripani M and Taiuti M 2024 *Nucl. Instrum. Meth. A* **1068** 169744

[37] He L X 2023 *Physics* **52** 476 (in Chinese)

[38] Heyd J, Scuseria G E and Ernzerhof M 2003 *J. Chem. Phys* **118** 8207

[39] Heyd, J and Scuseria G E 2004 *J. Chem. Phys* **121** 1187

[40] Adamo C and Barone V 1999 *J. Chem. Phys* **110** 6158

[41] Perdew J P, Ernzerhof M, Burke K 1996 *J. Chem. Phys* **105** 9982

[42] Nickerson B S, Liao W T and Pálffy A 2018 *Phys. Rev. A* **98** 062520

[43] Pimon M, Gugler J, Mohn P, Kazakov G, Mauser N and Schumm T 2020 *J. Phys.: Condens. Matter* **32** 255503

[44] Pimon M, Mohn P and Schumm T 2022 *Adv. Theor. Simul* **5** 2200185

[45] Bothwell T, Kedar D, Oelker E, Robinson J M, Bromley S L, Tew W L, Ye J and Kennedy C 2019 *Metrologia* **56** 065004

[46] Guan M, Bartokos M, Beeks K, Fujimoto H, Fukunaga Y, Haba H, Hiraki T, Kasamatsu Y, Kitao S, Leitner A, Masuda T, Nagasawa N, Okai K, Ogake R, Pimon M, Pressler M, Sasao N, Schaden F, Schumm T, Seto M, Shigekawa Y, Shimizu K, Sikorsky T, Tamasaku K, Takatori S, Watanabe T, Yamaguchi A, Yoda Y, Yoshimi A and Yoshimura K 2026 *Phys. Rev. Lett.* **136** 013203

[47] Dicke R H 1953 *Phys. Rev.* **89** 472

[48] Berengut J C, Dzuba V A, Flambaum V V and Porsev S G 2009 *Phys. Rev. Lett.* **102** 210801

[49] Rohde M and Salomon D 1983 *Hyperfine Interactions* **15** 257

[50] Von Der Wense L and Zhang C 2020 *Eur. Phys. J. D* **74** 146

[51] Ramakrishna J 1966 *Philos. Mag.* **13** 515

[52] Roesch L P, Kulessa R and Horber F 1975 *Phys. Status Solidi B* **71** 389

[53] Ooi T, Doyle J F, Zhang C, Higgins J S, Ye J, Beeks K, Sikorsky T and Schumm T 2025 arXiv:2507.01180

[54] Perera U C, Morgan H W T, Hudson E R and Derevianko A 2025 arXiv:2503.20984

[55] Morgan H W T, Terhune JE S, Elwell R, Bao Tran Tan H, Perera U C, Derevianko A, Hudson E R and Alexandrova A N 2025 arXiv:2503.11374

[56] Tkalya E V 2000 *Jetp Lett.* **71** 311

[57] Nienhuis G and Alkemade C T J 1976 *Physica B+C* **81** 181

[58] Rikken G and Kessener Y 1995 *Phys. Rev. Lett.* **74** 880

[59] Hiraki T, Okai K, Bartokos M, Beeks K, Fujimoto H, Fukunaga Y, Haba H, Kasamatsu Y, Kitao S, Leitner A, Masuda T, Guan M, Nagasawa N, Ogake R, Pimon M, Pressler M, Sasao M, Schaden F, Schumm T, Seto M, Shigekawa Y, Shimizu K, Sikorsky T, Tamasaku K, Takatori S, Watanabe T, Yamaguchi A, Yoda Y, Yoshimi A and Yoshimura K 2024 *Nat. Commun.* **15** 5536

[60] Terhune J E S, Elwell R, Tran Tan H B, Perera U C, Morgan H W T, Alexandrova A N, Derevianko A and Hudson E R 2024 arXiv: 2412.08998

[61] Schaden F, Riebner T, Morawetz I, De Col L T, Kazakov G A, Beeks K, Sikorsky T, Schumm T, V Lal K Z, Zitzer G, Tiedau J, Okhapkin M V and Peik E 2025 *Phys. Rev. Res.* **7** L022036